Hindawi Publishing Corporation
Advances in Meteorology
Volume 2015, Article ID 286206, 14 pages
http://dx.doi.org/10.1155/2015/286206

Research Article

Estimation of Continental-Basin-Scale Sublimation in the Lena River Basin, Siberia

Kazuyoshi Suzuki,[1] Glen E. Liston,[2] and Koji Matsuo[3]

[1]*Department of Environmental Geochemical Cycle Research, Japan Agency for Marine-Earth Science and Technology (JAMSTEC), 3123-75 Showamachi, Kanazawa-ku, Yokohama 236-0001, Japan*
[2]*Cooperative Institute for Research in the Atmosphere (CIRA), Colorado State University, Fort Collins, CO 80523-1375, USA*
[3]*Geospatial Information Authority of Japan, 1 Kitasato, Tsukuba, Ibaraki 305-0811, Japan*

Correspondence should be addressed to Kazuyoshi Suzuki; skazu@jamstec.go.jp

Received 9 September 2014; Accepted 18 December 2014

Academic Editor: Sven-Erik Gryning

The Lena River basin in Siberia produces one of the largest river inflows into the Arctic Ocean. One of the most important sources of runoff to the river is spring snowmelt and therefore snow ablation processes have great importance for this basin. In this study, we simulated these processes with fine resolution at basin scale using MicroMet/SnowModel and SnowAssim. To assimilate snow water equivalent (SWE) data in SnowAssim, we used routine daily snow depth data and Sturm's method. Following the verification of this method for SWE estimation in the basin, we evaluated the impact of snow data assimilation on basin-scale snow ablation. Through validation against MODIS snow coverage data and *in situ* snow survey observations, we found that SnowAssim could not improve on the original simulation by MicroMet/SnowModel because of estimation errors within the SWE data. Vegetation and accumulated snowfall control the spatial distribution of sublimation and we established that sublimation has an important effect on snow ablation. We found that the ratio of sublimation to snowfall in forests was around 26% and that interannual variation of sublimation modulated spring river runoff.

1. Introduction

Snow is one of the most important factors in the climate system of cold regions because of its high albedo and low heat conductivity [1–12], and it is also an important water resource in arid climates. On northern continental watershed scales, it is very important to evaluate snow mass in early spring for the prediction of snowmelt floods and hence there have been many studies on both snow accumulation and melt under various climatic conditions from point to global scales [2, 13–32].

Problems exist in relation to snow estimation because of difficulties in satellite-based measurements of snow mass. For instance, Foster et al. [33] reported a large error in radiance retrieval from a Siberian taiga forest because of the forest canopy. Point-scale snow surveys are more accurate than snow models or satellite retrievals; however, it is difficult to extend such surveys to larger scales, such as that of a continental basin. To estimate continental-basin-scale snow distribution, forcing variables for a land surface model are very important, and there are two principal methods by which to obtain such variables over a domain. One introduces independent datasets such as reanalysis data and the second interpolates surface meteorological data across the domain. Both methods have specific advantages and disadvantages.

Liston and Hiemstra [34] evaluated changes of pan-Arctic snow coverage over 30 years using their developed MicroMet/SnowModel and SnowAssim model with 10 km gridded forcing variables from NASA's Modern-Era Retrospective Analysis for Research and Applications (MERRA) reanalysis data [35], and they successfully detected snow mass trends in the Arctic region. Stuefer et al. [36] demonstrated that *in situ* snow observation was useful for the evaluation of snow distributions over a large domain in Arctic Alaska.

They used the SnowAssim model with meteorological station data to evaluate these distributions and demonstrated the effectiveness of *in situ* snow survey data in overcoming the limited meteorological forcing in the Arctic. Their research clearly showed that point-scale snow observations could improve the accuracy of large-scale snow distributions.

Routine measurements of snow water equivalent (SWE) are rarely available at high latitudes, but daily snow depth measurements from weather stations are available instead. Sturm et al. [37] developed empirical methods to determine SWE using snow depth data. Based on their method, Reichle et al. [38] estimated SWE in the Northern Hemisphere to validate their MERRA land products. However, Sturm's method could not be validated against Siberian snow data because the original validation dataset covered only North America and Europe. Thus, it is important to evaluate the applicability of Sturm's method to the vast region of Siberia.

Peterson et al. [39] reported that the annual river runoff for the six largest basins on the Eurasian continent increased by $2.0 \pm 0.7\,\mathrm{km}^3$ annually from 1936 to 1999. Rawlins et al. [40] showed that annual river runoff for the three largest Eurasian basins (the Ob, Yenisei, and Lena) correlated well with cold season (October–April) precipitation from 1966 to 1995. In addition, Kitaev et al. [41] demonstrated that the snow mass over the region of the former Soviet Union increased from 1936 to 1995. In the Lena River basin, Iijima et al. [42] showed that an abrupt increase in active layer depth had a positive correlation with precipitation increase. Furthermore, they described the role of snow as an insulator for the permafrost. However, there were very limited observations of snow depth and the study did not reflect basin-scale snow mass change. In the upper Lena River basin, Suzuki et al. [43, 44] showed that snow mass strongly affected the river runoff ratio and organic carbon transport. The Lena River is the second largest provider of freshwater from the land to the Arctic Ocean. Freshwater discharge and organic carbon from the river can modulate sea ice production, ocean circulation, and ecosystem. Estimation of snow mass in the Lena River basin is also important for the evaluation of freshwater and carbon transport to the Arctic Ocean. In order to estimate snow mass, Zhang et al. [45] and Suzuki et al. [46] clarified the importance of sublimation in the winter water balance. The ratio of sublimation loss to total winter snowfall ranged from 20% to 50% in the region. However, their research was limited to a small-scale watershed, and thus it is unclear which factors affect the spatial distribution of sublimation on the scale of the Lena River basin.

At high latitudes, meteorological stations are sparse and located mostly at low elevations. Thus, reanalysis data from operational weather centers have uncertainties and relatively large errors in comparison with data from the midlatitudes of the Northern Hemisphere. Estimations using snow data assimilation provide information on changes of both solid precipitation and active layer processes. These changes ultimately modify the water balance components in permafrost regions. Here, through estimation of SWE from daily routine snow depth data from weather stations, we show the effect of simple snow data assimilation on the water balance of the permafrost-dominated Lena River basin. In addition, we clarify the spatial distribution of sublimation and its role in snow ablation processes.

2. Methodology

2.1. Study Domain and Forcing Variables. The topography and vegetation distribution of the study area are shown in Figures 1(a) and 1(b), respectively. The domain size of about 2,500 × 2,000 km (50°N–74°N, 110°E–165°E) required about 1.493 million 2 km grid cells for the model simulations. The study area encompasses the Lena River basin, which has an area of about $2{,}500{,}000\,\mathrm{km}^2$ and generates one of the largest river inflows to the Arctic Ocean. The Lena River flows 4,400 km from its source in mountainous southeastern Siberia to its mouth in the Arctic Laptev Sea. The mountainous areas in the basin have gentle slopes with the highest elevation of around 1,300 m. Most of the basin is relatively flat from the middle to lower reaches. We used digital elevation data (GTOPO30 [47]) and converted the original 30-second grid cells into 2 km cells using ArcGIS 9.2 software.

We used the GLC2000 dataset to set up the vegetation classification within the domain [48]. The original GLC2000 vegetation map had 1 km grid cells, but we converted it into 2 km cells with 18 vegetation classifications, which were required for the model parameters of MicroMet/SnowModel. Figure 1(b) and Table 1 show the vegetation distribution within the domain. The major vegetation types were forest and tundra and forest comprised 80% of the area of the Lena River basin. Within this forest, deciduous trees that were mainly larch were predominant.

2.2. Dataset. Here, we describe the details of the forcing and validation datasets used for the simulations. First, for the forcing variables, we used the baseline meteorological dataset (BMDS) archived by [49] and distributed at http://www.jamstec.go.jp/acdap/Summary.action?downloadList=A20100830-001&selectFile=A20100830-001. The stations in the BMDS are mostly at low elevations and latitudes, as shown in Figure 1(a). Thus, meteorological data from high elevations and latitudes within the domain were very limited. The number of meteorological stations used for the simulations was 47, and the meteorological data were daily mean air temperature, relative humidity, wind speed, precipitation, and snow depth. Therefore, the time step implemented in the simulations was one day. All data were quality controlled and, in particular, precipitation data were modified carefully based on station-specific parameters of wind-induced precipitation gauge undercatch, which causes underestimation of winter precipitation [50].

Second, to assimilate SWE data in the model, we used *in situ* snow survey observations from two snow courses in mid-March 2000. In that month, the National Polar Research Institute of Japan performed two snow survey courses, and the locations of the snow observation are shown in Figure 1(a) and Table 2. These once-per-year snapshots of observed snow data included snow depth, snow density, and SWE.

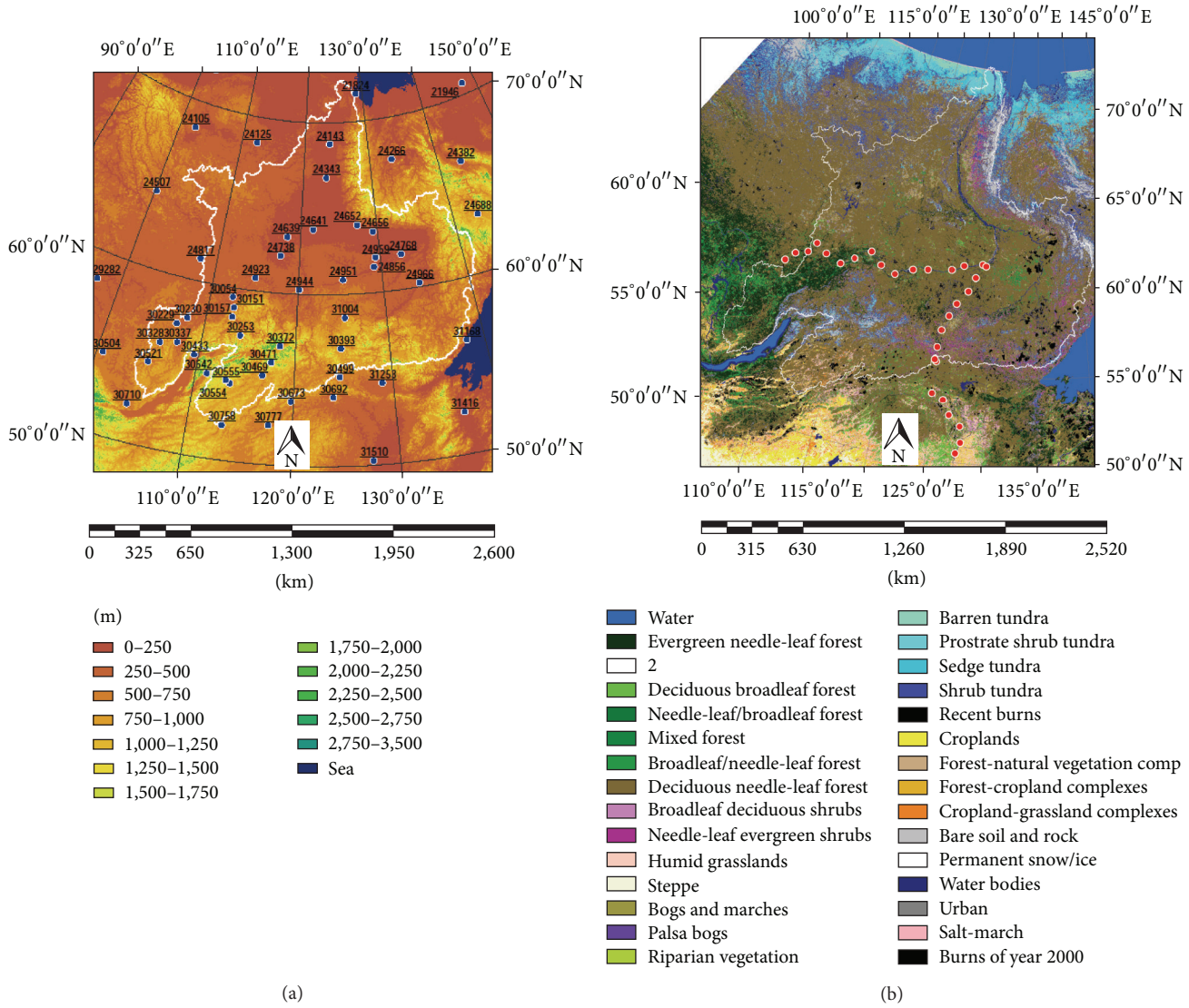

FIGURE 1: Location of study site with (a) topography and (b) vegetation classification. Blue circles in panel (a) denote locations of BMDS sites. Red circles in panel (b) show locations of *in situ* observation sites of the National Polar Research Institute of Japan.

Finally, to verify the spatial distributions of model estimates, we used monthly composite MODIS MOD10 snow coverage products with 0.05° resolution. We used these products to overcome the problem of missing snow coverage information in the eight-day composite data. We converted our simulated results from 2 km to 0.05° resolution for comparison with the MOD10 snow products.

2.3. Sturm's SWE Estimation. SnowAssim requires SWE data, but the weather stations used in this study routinely only report daily snow depths. Therefore, we estimated SWE from the snow depth data using the following method developed by [37], which has snow depth observation and climate snow classes. The basic equation for estimating SWE can be written as follows:

$$\mathrm{SWE} = \rho_{h,\mathrm{DOY}_i} \times \frac{h_s}{\rho_w}, \tag{1}$$

$$\rho_{h,\mathrm{DOY}_i} = (\rho_{\max} - \rho_0)\left[1 - \exp\left(-k_1 \times h_i - k_2 \times \mathrm{DOY}_i\right)\right] + \rho_0, \tag{2}$$

where ρ_{h,DOY_i} is bulk snow density for snow depth h_s and day of the year (DOY_i); ρ_w is water density; k_1 and k_2 are densification parameters for depth h_s and DOY_i, respectively; and $\rho_{\max}$,ρ_0, k_1, and k_2 are parameters that vary with snow class.

To examine the accuracy of SWE estimated using Sturm's method, we compared it with *in situ* snow observations

Table 1: Vegetation types in study area and river basin.

Vegetation class	Vegetation description	Percentage of total study area (%)	Percentage of total river basin area (%)
Forest	Coniferous forest	6.8	7.4
	Deciduous forest	49.3	61.1
	Mixed forest	2.1	2.9
	Scattered short-conifer	3.0	3.2
	Clearcut conifer	1.8	2.1
Shrub	Mesic upland shrub	0.4	0.2
	Xeric upland shrub	0.2	0.1
	Playa shrubland	2.3	3.6
	Shrub wetland/riparian	0.1	0.0
	Erect shrub tundra	5.7	3.6
	Low shrub tundra	3.9	1.3
Grass	Grassland rangeland	0.8	0.7
	Subalpine meadow	0.5	0.6
	Tundra (nontussock)	0.0	0.0
	Tundra (tussock)	9.6	6.2
	Prostrate shrub tundra	1.0	0.1
	Arctic grassy wetland	2.1	1.2
Bare	Bare	4.0	3.5
	Water/possibly frozen	5.9	1.6
	Permanent snow/glacier	0.0	0.0
	Residential/urban	0.0	0.0
	Tall crops	0.5	0.3
	Short crops	0.4	0.3
Total area		5,970,000 km^2	2,500,000 km^2

(Table 2). Figure 2 shows a comparison of observed and estimated SWE at *in situ* observation sites. There is a clear linear relationship with a large determination coefficient. The slope of the linear regression is close to 1 and the root mean square error (RMSE) is about 24 mm, lower than that of the original paper [37]. Thus, we believe that Sturm's SWE method is applicable to our study domain. However, the RMSE tends to become larger at higher values of SWE, and Sturm's method usually provides an overestimate.

2.4. Model and Data Assimilation. Here, we describe the MicroMet/SnowModel [51, 52] and SnowAssim model [53] that we used to simulate snow distributions and water and energy balances at each grid cell of the domain.

MicroMet/SnowModel is a comprehensive snow-evolution modeling system that includes blowing snow transport processes [51, 52]. This system contains all the physics and dynamics required to simulate snow evolution in both forested and nonforested environments. SnowModel incorporates the first-order physics required to simulate snow evolution in each global snow class (i.e., ice, tundra, taiga, alpine/mountain, prairie, maritime, and ephemeral), as

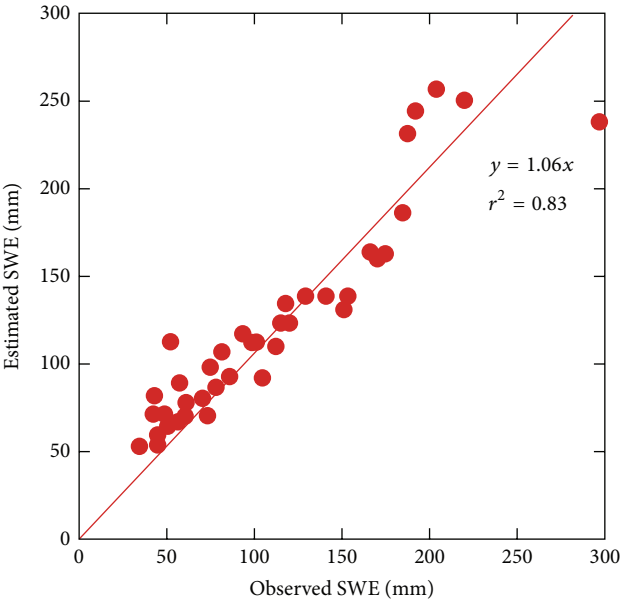

Figure 2: Comparison of SWE by Sturm's estimation with *in situ* observation by the National Polar Research Institute of Japan.

Table 2: Snow observation sites and observed data (NA indicates no data).

Site name	Observation date	Latitude (°)	Longitude (°)	Elevation (m)	Snow depth (m)	Snow water equivalent (mm)	Density (kg m^{-3})
YKS	Mar 13, 2000	129.664E	62.009N	100	NA	48	NA
YI1	Mar 14, 2000	128.502E	61.283N	110	0.25	86	178
YI2	Mar 14, 2000	126.388E	61.094N	120	0.43	157	202
YI3	Mar 15, 2000	125.030E	60.776N	130	0.64	98	239
YI4	Mar 15, 2000	122.318E	60.563N	165	0.39	97	252
YI5	Mar 16, 2000	120.661E	60.390N	145	0.54	75	173
YI6	Mar 16, 2000	106.768E	57.805N	135	0.43	44	199
YI7	Mar 17, 2000	106.523E	57.284N	265	0.27	213	168
YI8	Mar 17, 2000	105.289E	56.803N	145	0.84	172	262
YI9	Mar 17, 2000	105.027E	56.740N	185	0.86	190	215
YI10	Mar 18, 2000	102.683E	56.411N	415	0.86	137	237
YI11	Mar 19, 2000	101.216E	56.130N	325	0.64	100	202
YI12	Mar 19, 2000	101.255E	54.433N	500	0.52	171	194
YI13	Mar 19, 2000	102.671E	53.444N	540	0.82	168	234
YI14	Mar 20, 2000	104.760E	51.945N	460	0.75	117	233
YI15	Mar 20, 2000	106.768E	57.805N	515	0.57	171	202
YI16	Mar 21, 2000	106.523E	57.284N	530	0.73	51	238
YI17	Mar 21, 2000	105.289E	56.803N	330	0.32	95	161
YI18	Mar 22, 2000	105.027E	56.740N	335	0.49	149	192
YI19	Mar 22, 2000	102.683E	56.411N	530	0.62	130	241
YI20	Mar 22, 2000	101.216E	56.130N	525	0.65	131	198
YI21	Mar 23, 2000	101.255E	54.433N	555	0.58	51	225
YI22	Mar 23, 2000	102.671E	53.444N	545	0.29	89	172
YI23	Mar 24, 2000	104.760E	51.945N	500	0.49	62	180
YI24	Mar 25, 2000	106.768E	57.805N	100	0.28	48	225
YH1	Mar 16, 2000	128.923E	61.190N	220	0.61	151	250
YH2	Mar 16, 2000	127.871E	60.503N	480	0.57	120	210
YH3	Mar 16, 2000	127.206E	59.693N	350	0.62	118	190
YH4	Mar 17, 2000	126.118E	58.919N	300	0.76	166	220
YH5	Mar 17, 2000	125.473E	58.189N	980	1.10	297	270
YH6	Mar 17, 2000	124.905E	57.351N	1100	0.78	187	240
YH7	Mar 18, 2000	124.720E	56.373N	960	0.74	170	230
YH8	Mar 18, 2000	124.835E	55.558N	630	0.64	141	220
YH9	Mar 18, 2000	124.653E	55.676N	720	0.51	112	220
YH10	Mar 19, 2000	124.868E	53.767N	450	0.36	61	170
YH11	Mar 19, 2000	125.969E	53.459N	450	0.30	51	170
YH12	Mar 19, 2000	126.686E	52.643N	380	0.31	56	180
YH13	Mar 20, 2000	127.776E	52.052N	200	0.37	70	190
YH14	Mar 20, 2000	127.974E	51.153N	200	0.37	81	220
YH15	Mar 20, 2000	127.608E	50.526N	200	0.34	75	220

defined by [54]. MicroMet and SnowModel have been used to distribute meteorological variables and evolve snow distribution over a wide range of spatial scales (grid increments ranging from 10 m to 10 km and spatial domains from 100 m to pan-Arctic). The models have been used for a variety of complex landscapes, including the mountains of Colorado, Wyoming, Idaho, Arctic Alaska, Svalbard, Central Norway, Greenland, and Japan.

SnowModel incorporates four submodels: MicroMet [51], which defines meteorological forcing conditions; EnBal [55], which calculates surface energy exchanges; SnowPack [52], which simulates snow depth and water equivalent evolution;

and SnowTran-3D [56], which accounts for snow redistribution by wind. Each submodel was originally developed and tested for nonforested conditions. For application to Japanese forest areas, the submodels have been modified by Suzuki et al. [57], using the model and measurements [58].

Next, we describe the simple snow data assimilation method (SnowAssim) [53]. This method requires plausible plot-scale SWE data. Based on the differences between the simulated and these plausible SWE data, SnowAssim modifies either the precipitation or melt from SnowModel. This is performed by calculating the relative contributions (R) of precipitation and melt during each observation interval using the following:

$$ {}_{t-1}^{t}R_{\text{prec}} = \frac{\sum_{t-1}^{t} P}{\sum_{t-1}^{t} P + \sum_{t-1}^{t} M}, \tag{3} $$

$$ {}_{t-1}^{t}R_{\text{melt}} = 1 - {}_{t-1}^{t}R_{\text{prec}}, \tag{4} $$

where P and M are accumulated precipitation and snowmelt from times $t-1$ to t, respectively. The greater of these defines whether it is precipitation or melt that is corrected. During periods in which there are no future observations, or in which both the summed precipitation and melt are zero, the correction factor is defined as unity. An additional requirement of our data assimilation system is that it be spatially distributed.

2.5. Experiments

2.5.1. Snow Data Assimilation Experiment. To evaluate the basin-scale impact of estimated SWE on routine snow depth observations in our model simulation, we performed two simulations targeting the winter of 1999–2000. In this period, both MODIS snow cover products and *in situ* snow observations were available and we verified the simulated results with those data. Firstly, we executed a control run for September 1, 1999, to August 31, 2000, without snow data assimilation in the model, hereafter, called the CTL9900 run. Secondly, we performed the same simulation, but incorporating snow data assimilation using SWE estimated by Sturm's method, hereafter, called the ANL9900 run. The estimated SWE was based on daily snow depth data observed by BMDS weather stations. For the snow data assimilation, we chose data at 10-day intervals from September 1, 1999, to August 31, 2000. For each 10-day period, we estimated the SWE at the BMDS sites from our routine snow depth observations and those SWE data were assimilated into SnowAssim.

2.5.2. Multiyear Snow Process Experiment. To evaluate the snow ablation processes in different years, we performed multiyear snow simulations for September 1, 1998, to August 31, 1999, and September 1, 1999, to August 31, 2000. The regulation in the latter period was the same as in the CTL9900 run. We refer to the simulation of winter 1998–1999 as the CTL9899 run. Based on these two simulations, we evaluated the variation of the snow processes in different years.

3. Results and Discussion

3.1. Hydrometeorological Conditions in the Two Winters. We show here the hydroclimatic conditions in the Lena River basin during the study periods of the two winters of 1998–1999 and 1999–2000. Figures 3(a)–3(d) show the monthly variations of hydrometeorological conditions using the average of all the BMDS stations shown in Figure 1(a), from September 1998 to August 2000. Vertical error bars denote standard deviations of each factor among the BMDS sites. Most river runoff occurred during spring (April through June) (Figure 3(a)). This runoff commenced in May of both years and the accumulated river runoff from October through the following June in each year was 122 and 146 mm, respectively; that is, runoff in winter 1999–2000 was 24 mm greater than in 1998–1999. In accordance with this difference in runoff, winter precipitation in 1999–2000 was 20 mm greater than in 1998–1999. Precipitation had clear interannual variations with maxima recorded in summer. Therefore, the difference in river runoff between the two winters was largely caused by the difference in precipitation.

Figure 3(b) reveals the extent of the extremely cold winter air temperatures; for example, the monthly mean air temperature for January is around −30°C. Mean air temperature for October through June in 1998–1999 (−17.5°C) was lower than in 1999–2000 (−16.2°C), and the colder winter of 1998–1999 extended the snow period compared with winter 1999–2000. However, maximum snow depth in both years was similar (Figure 3(e)), which suggests that snowfall did not differ much between the two winters.

3.2. Effect of Data Assimilation on Estimated SWE from Weather Stations. In this section, we assess model performance and the effectiveness of snow data assimilation relative to other independent observations, that is, MODIS satellite-retrieved snow coverage and plot-scale *in situ* snow observations.

First, to demonstrate the basin-scale spatial performance of the simulated snow distribution, we compare the two sets of snow coverage simulated by CTL9900 and ANL9900 with satellite-retrieved monthly composite MODIS snow data [59]. Here, we converted the original 2 km gridded simulation results to 0.05° resolution to match the gridded MODIS data. Figures 4(a)–4(c) show the spatial distributions of monthly snow coverage by MODIS, CTL9900, and ANL9900, respectively. It can be seen that there is no significant difference between these and April 2000, as shown in Figures 4(a), 4(b1), and 4(c1). Figures 4(a1), 4(b1), and 4(c1) show that in April all three datasets indicate that most of the basin was covered by snow. In May, the difference between CTL9900 and ANL9900 is significant, because the latter indicates snow persisted in the high mountain areas of the upper Lena River basin and that Sturm's method [37] for snow data assimilation overestimated the SWE, a trend confirmed by Figure 2. The results showed that the CTL9900 simulation was closer than ANL9900 to the MODIS observations (spatial correlations between MODIS and the CTL9900 and ANL9900 simulations were 0.69 and 0.58, resp.). In June 2000, all three results were similar because much of the

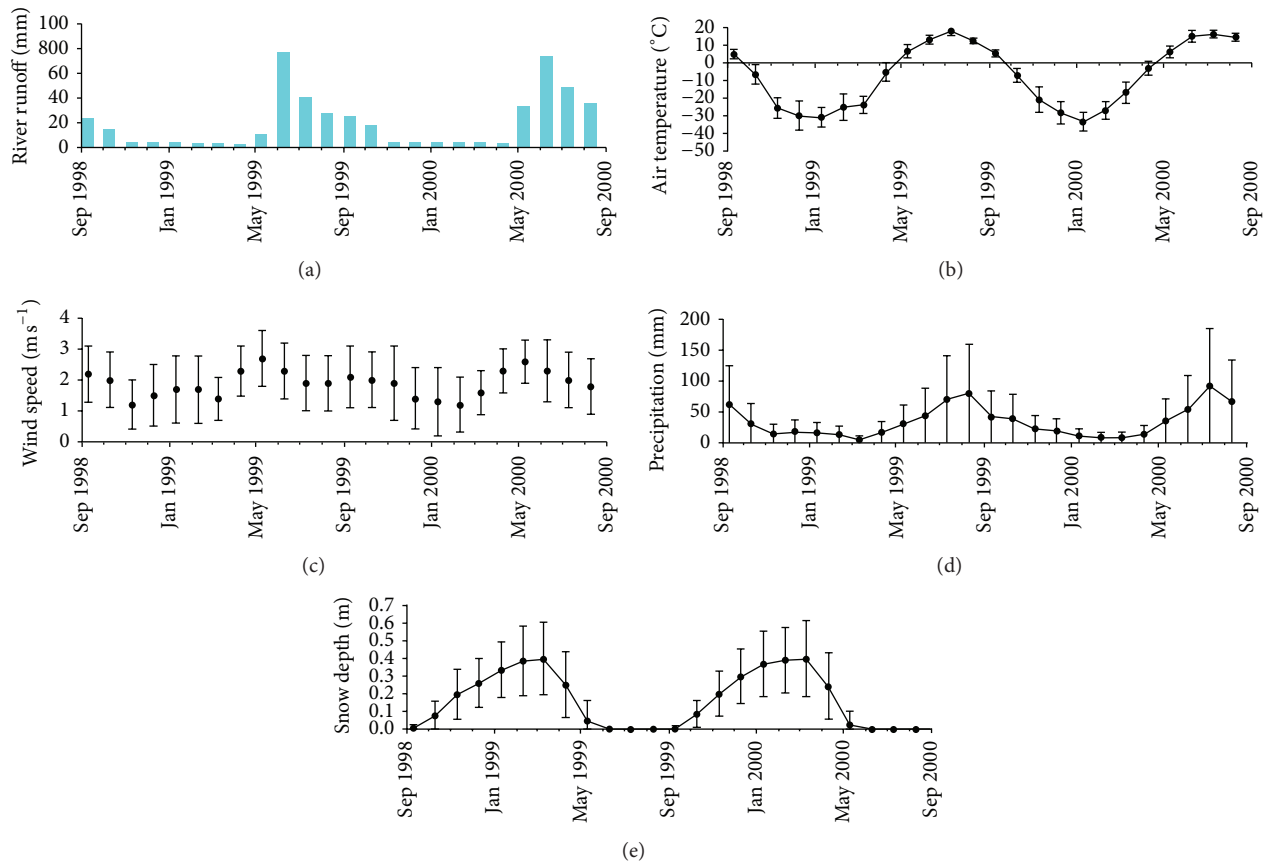

Figure 3: Monthly variations of hydrometeorological conditions. (a) River runoff at mouth of Lena River basin, (b) air temperature, (c) wind speed, (d) precipitation, and (e) snow depth.

snow coverage had disappeared, although the snow coverage simulated by ANL9900 was larger than that of either MODIS or CTL9900. In Section 2.3, we highlighted that SWE from Sturm's method is an overestimation for higher values of SWE. The overestimation by ANL9900 was caused by the assimilation of overestimated SWE in the upper Lena River basin. In turn, overestimated SWE affected estimated daily precipitation and thus winter precipitation from ANL9900 was poorer than that of the original model run by CTL9900. Overall, we conclude that large errors in the estimation of SWE in the data assimilation lead to poorer simulation results. However, in Section 3.4, we also consider possible problems with the MODIS snow products, because MODIS satellite-retrieved snow coverage includes uncertainties in its retrievals and therefore it requires ground truth.

Next, we compare the simulated and observed SWE at point-scale for the *in situ* snow observation sites shown in Figure 1(b). Figures 5(a) and 5(b) show comparisons of observed and simulated SWE at these sites (listed in Table 1). Figure 5(a) shows a clear linear relationship between the *in situ* observations and CTL9900 simulation with a slope of 1.03, large determination coefficient of 0.46, and RMSE of 44 mm. In contrast, the relationship between the observations and ANL9900 is unclear and has larger discrepancies. The determination coefficient of 0.22 is smaller and the RMSE of 89 mm is nearly double that of CTL9900. As shown in Figure 4(c), the snow coverage simulated by ANL9900 remained in the upper Lena River basin. The results shown in Figures 5(a) and 5(b) correspond to those in Figures 4(b) and 4(c). One of the reasons for the large difference between the observations and the SWE simulated by ANL9900 (Figure 5(b)) was the overestimation of SWE by Sturm's method. This is because SnowAssim corrected the precipitation at the BMDS sites, which are mainly located at lower elevations, in order to match the overestimated SWE, and the corrected precipitation was interpolated to the grid points with the inclusion of orographic effects. Therefore, the SWE estimated for higher elevations by ANL9900 was enhanced by orographic effects of precipitation, derived from overestimations of SWE at lower elevations.

Routine snow depth data for SWE were also measured at the weather stations. As mentioned in Section 2.2, the BMDS precipitation was quality controlled for research purposes and calibrated by empirical wind-induced undercatch parameters for each station. Thus, we believe that the quality of the estimated SWE input into SnowAssim was poorer than that of the winter precipitation, owing to the sophisticated BMDS precipitation, which resulted in no improvement in the SnowAssim simulation.

Another consideration is that the BMDS stations were mainly at lower elevations and latitudes. At higher elevations and latitudes, forcing meteorological variables were estimated

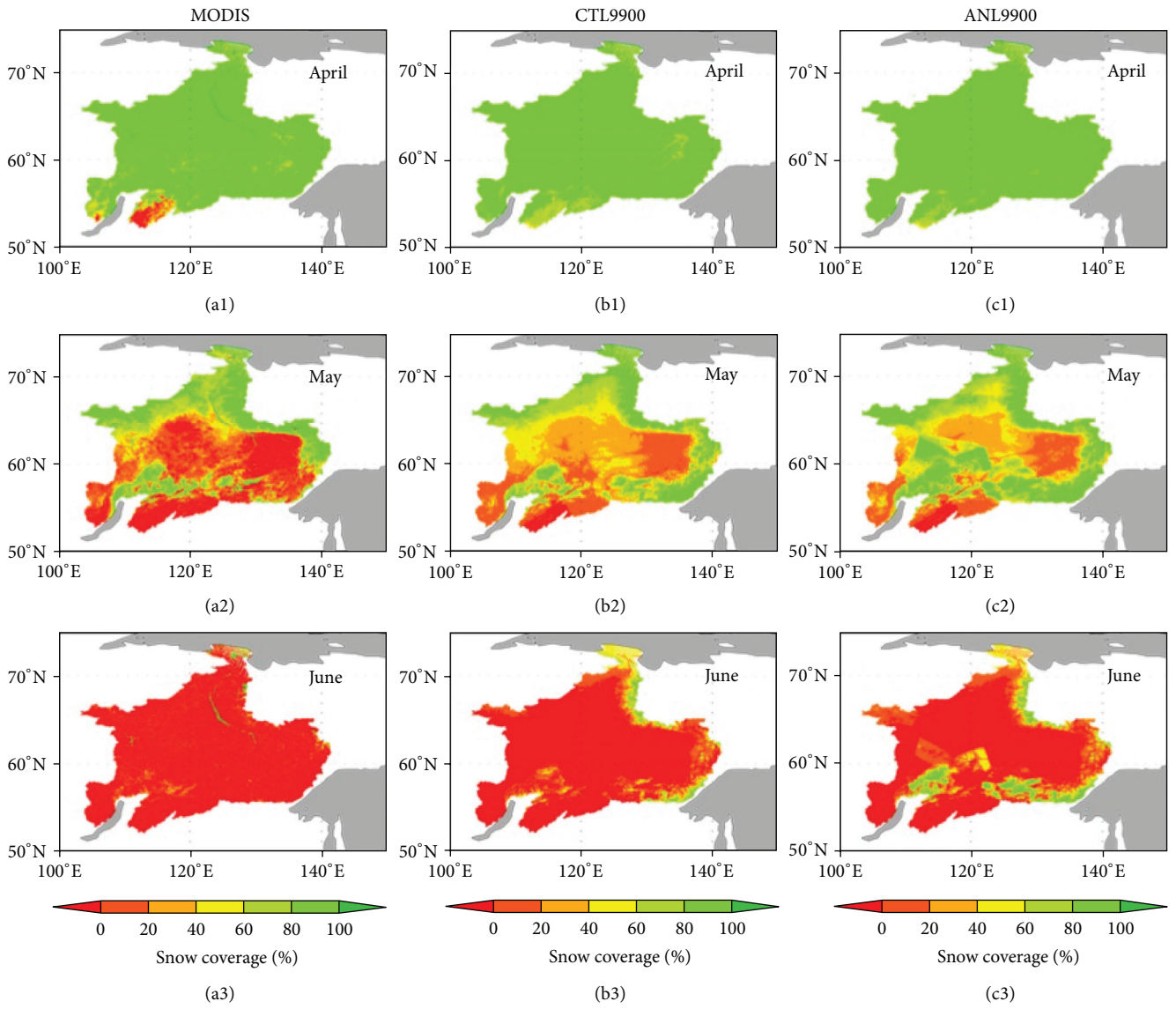

Figure 4: Validation of spatial distribution of basin snow coverage with monthly MODIS products. (a1–a3) MODIS snow products in April, May, and June 2000, respectively. (b1–b3) Simulated results of CTL9900 in the same months as (a). (c1–c3) Simulated results of ANL9900 in the same months as (a).

by the MicroMet model using Barnes' objective interpolation method [60]. Here, when we excluded orographic effects on air temperature, the disappearance of simulated snow coverage was much faster than with the MODIS snow coverage dataset. We also tested the exclusion of orographic effects on precipitation in MicroMet. The simulation results were similar to those of the exclusion of orographic effects on air temperature; snow disappearance was much faster than with the MODIS snow coverage dataset. Thus, despite most of the BMDS being obtained from lower elevations and latitudes, the proper treatment of orographic effects on air temperature and precipitation meant that the results of CTL9900 were closer to the MODIS snow coverage.

Overall, the simulated results of CTL9900 were superior to those of ANL9900. This was because of the overestimations of SWE and winter precipitation in ANL9900, especially at high elevations. Thus, we believe that the control run without data assimilation can reproduce snow processes on the basin scale reasonably well. In the subsequent analysis of the winter water balance, we used only the control run for 1998–1999 and 1999–2000.

3.3. Sublimation in the Lena River Basin. Suzuki et al. [57] and Zhang et al. [45] showed that sublimation was important for point-scale water balance during a winter in the upper Lena River basin. Here, we show the distribution of sublimation across the basin and the main spatially controlling factors.

First, we show spatial variations in each winter's water balance components from September 1 to the end of July the following year. Figures 6(a)–6(d) show the spatial variations of each winter's accumulated water balance components

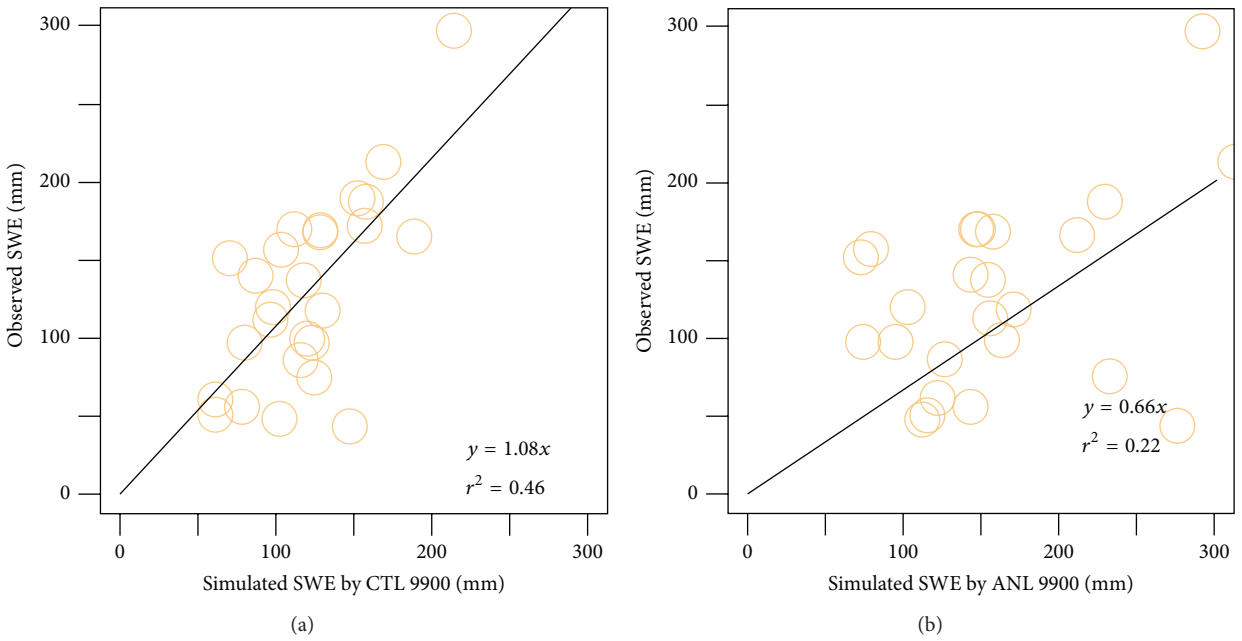

Figure 5: Point-scale validation of SWE with *in situ* snow observations and simulated results of (a) CTL9900 and (b) ANL9900.

(snowfall, sublimation, snowmelt, and ratio of sublimation to snowfall) in CTL9900 from September 1, 1999, to July 31, 2000. The range of accumulated snowfall was about 50 mm in the southern part of the upper Lena basin to more than 300 mm at higher elevations. In contrast, the range of accumulated sublimation in the basin was smaller (about 50–80 mm). Therefore, the ratio of accumulated sublimation to accumulated snowfall was of the order of about 0.1 to >0.5. Thus, in some parts of the basin, more than half the snowfall was lost to sublimation; these parts had little snowfall. At high elevations, snowfall was heavy and sublimation slight; therefore, the ratio of sublimation loss to snowfall was insignificant and melt dominated the snow ablation. This concurs with the result of Ma et al. [61], who demonstrated that the southern mountain area was the main source of river runoff in the basin.

Next, we examined which factors affected the basin-scale spatial distribution of sublimation. Table 3 presents the spatial correlation between accumulated sublimation from CTL9900 and various factors, which shows strong correlation between vegetation density and snowfall. Table 4 lists snow ablation components for different vegetation types (where tundra is classified as grass). It is clear that forest had less snowpack, strong sublimation, and less snowfall. Thus, net snow accumulation on the ground was smaller in comparison with other vegetation types. For those types, winter sublimation was 5–7 mm and the ratio of sublimation to snowfall was only 2-3%. Thus, sublimation is important to the winter water balance in forest regions. In other words, forest can limit the amount of snowpack because of the greater sublimation loss there. We believe that the forest distribution can be determined by the amount of snowpack, because deeper snowpack produces a surface water layer during snowmelt due to the frozen ground in permafrost areas. In addition, wet conditions might cause respiration difficulty for tree roots and thus forest would not survive under deeper snowpack in the permafrost region.

Table 3: Spatial correlations of various factors with accumulated sublimation in CTL9900.

Factors	Spatial correlation—sublimation	Spatial correlation—percentage of sublimation
Elevation	0.35	0.25
Vegetation density	0.86	0.86
Accumulated snowfall	−0.87	−0.92
Mean air temperature	−0.30	−0.20
Mean water vapor pressure	−0.36	−0.27

Note: wind speed and latitude had no correlation. All correlation coefficients were significant at the 0.01 level.

Table 4: Vegetation classes and mean accumulated sublimation in CTL9900.

Vegetation class	Snowfall (mm)	Accumulated sublimation (mm)	Percentage of sublimation loss to accumulated snowfall (%)
Forest	139	37	26.6
Shrub	229	5	2.2
Grass	213	7	3.3
Bare	206	5	2.4

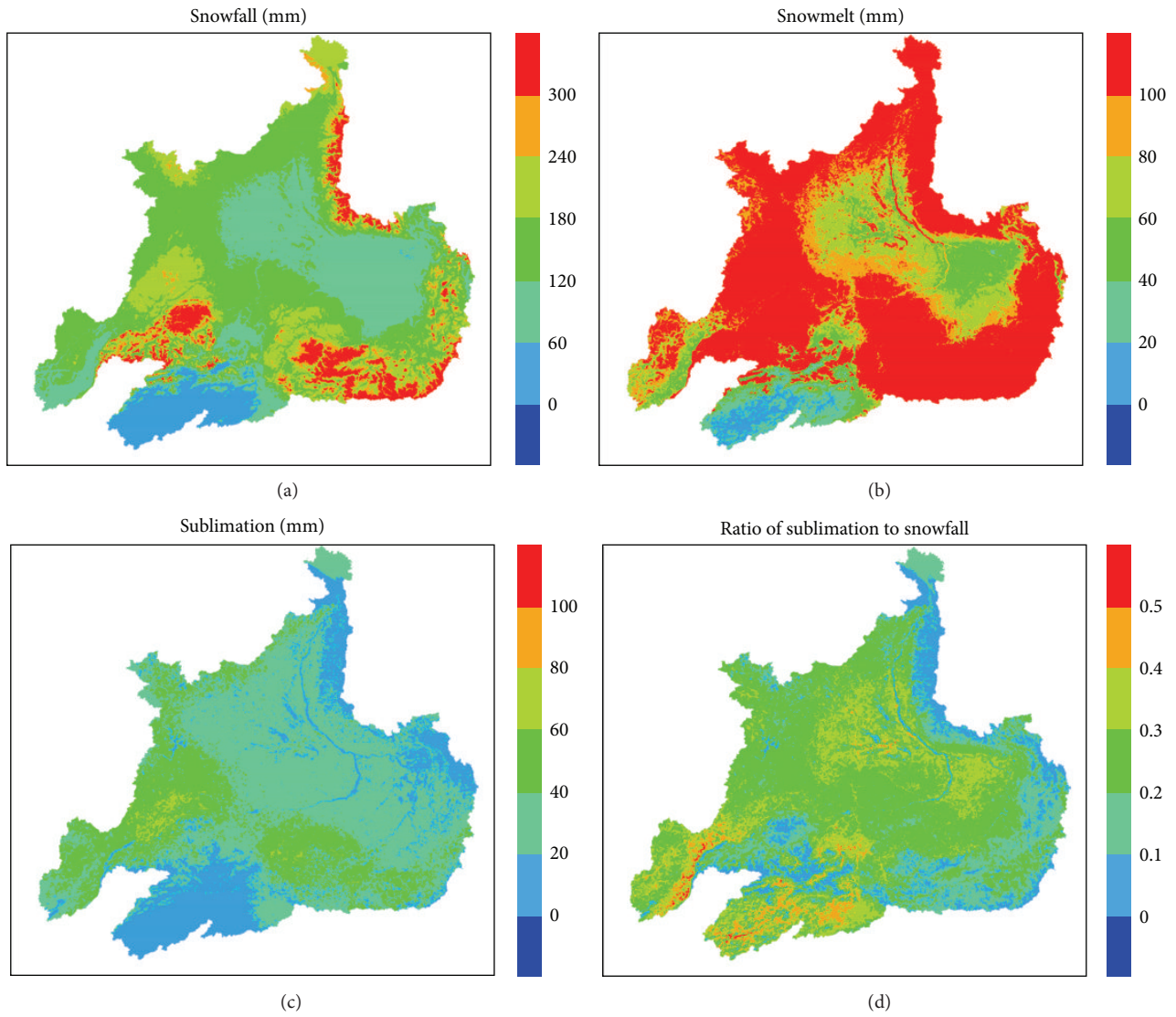

Figure 6: Spatial distribution of accumulated snowfall, snowmelt, sublimation, and ratio of sublimation to snowfall during winter 1999–2000 from CTL9900: (a) snowfall, (b) snowmelt, (c) sublimation, and (d) ratio of sublimation loss to total snowfall.

Table 5: Winter water balance and meteorological components in the basin in CTL9899 and CTL9900.

Year	Snowfall (mm)	Sublimation (mm)	Ratio of sublimation loss to snowfall (%)
CTL9899	179	29	16.2
CTL9900	162	24	14.8

Next, we investigated how interannual snow ablation processes in the two winters affected the water balance. As shown in Section 3.1, total precipitation in the winter of 1999–2000 was 20 mm greater than that of 1998–2000. Table 5 lists the water balance components for the two winters. Consistent with this table, snowfall from CTL9899 was about 15 mm greater than that of CTL9900 because of the colder climate in CTL9899, as shown in Figure 3(b). This colder climate caused a longer period of snow, as shown in Figure 7(a) compared with Figure 7(b). However, basin-scale average SWE did not differ between CTL9899 and CTL9900, although the accumulated sublimation from CTL9899 was 5 mm greater than that of CTL9900. Thus, the ratio of sublimation to snowfall from the former run was 16.2%, compared with 14.8% from the latter. This difference could explain the discrepancy in river runoff indicated in Section 3.1, because the difference of total precipitation alone could not explain the 5 mm water equivalent difference in river runoff. Thus, sublimation is important for estimating river runoff accurately, especially that which occurs in spring. Therefore, river runoff can be affected by interannual variation of sublimation within the basin.

3.4. Discussion. Firstly, our study period was limited to two years. Therefore, the contribution of sublimation to snow

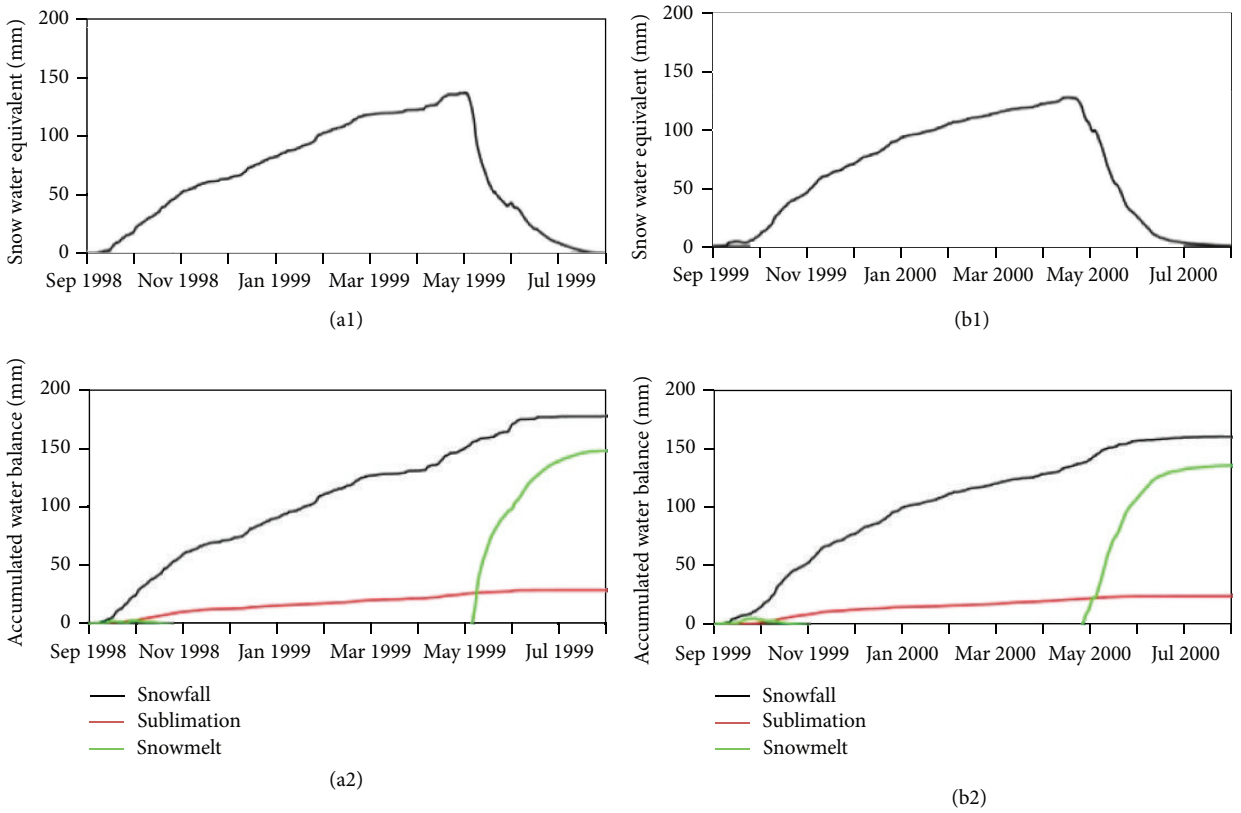

Figure 7: Temporal variations of basin-average water balance components and SWE: (a) winter 1998–1999 from CTL9899 and (b) winter 1999–2000 from CTL9900.

ablation could vary in response to different extreme climate conditions. However, our results are adequate for indicating the importance of sublimation in ablation processes within the region.

Secondly, MODIS snow coverage is based on satellite-based retrievals. Thus, the product itself has uncertainty and requires ground-truth observations to evaluate its accuracy. For example, Klein and Barnett [62] showed that MODIS typically misses snow coverage when its depth is less than 4 cm. Thus, another reason for the overestimation of snow coverage in CTL9900 and ANL9900 for May 2000 (Figures 4(b) and 4(c)) could be ascribed to the underestimation of snow coverage by the MODIS snow product, because the Lena River basin was largely covered by shallow snowpack due to the limited snowfall.

Thirdly, the representativeness of the BMDS stations is difficult to address because their locations are mostly at lower elevations and latitudes. Thus, our analysis would be improved if we had routine snow depth data from high mountain areas. Through the estimation of SWE with snow depth data, we believe that SnowAssim likely improved the simulations of snow mass and snow coverage over MicroMet/SnowModel. Therefore, our conclusion regarding SnowAssim might be limited to situations where there are routine snow depth and meteorological datasets available at the same locations.

Finally, we excluded blowing snow events in the simulations because each grid cell was 2×2 km, which means that blowing snow at that scale can be canceled by subgrid depositional and erosional effects. Nevertheless, blowing snow does cause sublimation [63] and it changes snow deposition on the ground. However, at high elevations, we saw no evidence of strong sublimation. With strong winds, the inclusion of blowing snow could enhance the sublimation and heterogeneity of the snow distribution within a grid cell. Thus, fine-scale phenomena such as blowing snow at subgrid scale could alter the contribution of sublimation. Further research should focus on the impact of blowing snow sublimation in windy areas of the Lena River basin.

4. Conclusions

Overall, we demonstrated the applicability of MicroMet/SnowModel and SnowAssim in poorly observed regions. The methods we employed are not restricted to the study area but could be applied to other poorly observed cold regions such as the Arctic, North Canada, Greenland, the Alps, or the Tibetan Plateau. In addition, our approach has benefits regarding the understanding of long-term trends of river runoff in large northern river basins.

In this study, we used MicroMet/SnowModel and SnowAssim in the Lena River basin area. In addition, we calculated SWE with routine snow depth observations from weather stations using Sturm's method [37] and assimilated the results in SnowAssim. We were able to draw the following conclusions.

(1) Sturm's method can be applied to the Lena basin area of eastern Siberia, within its original estimation error.

(2) Simulated snow coverage and distribution were verified against *in situ* observed snow data. SnowAssim did not improve the simulated results of MicroMet/SnowModel, because the SWE estimation error in SnowAssim was greater than the model error. Moreover, the BMDS precipitation was of good quality, in contrast to the quality of the estimated SWE.

(3) Basin-scale sublimation was important for components of the winter water balance. The spatial distribution of sublimation was determined primarily by vegetation and accumulated snowfall.

(4) Interannual variation of sublimation affected the amount of spring river runoff. Greater sublimation reduced river runoff because of reduced SWE on the ground.

Conflict of Interests

The authors declare that there is no conflict of interests regarding the publication of this paper.

Acknowledgments

The authors acknowledge Professor Emeritus Yoshiyuki Fujii of the National Polar Research Institute of Japan, who kindly provided the institute's *in situ* snow data from the Siberian region. Parts of this study were supported by Grants-in-Aid for Scientific Research (C) (no. 20510031), Grants-in-Aid for Challenging Exploratory Research (no. 25550022), the JAXA/GCOM-W Project (PI no. D11), and the GRENE Arctic Climate Change Research Project: The role of Arctic Cryosphere in Global Change (PI: Professor H. Enomoto).

References

[1] T. Yasunari, A. Kitoh, and T. Tokioka, "Local and remote responses to excessive snow mass over Eurasia appearing in the northern spring and summer climate–a study with the MRI GCM," *Journal of the Meteorological Society of Japan*, vol. 69, pp. 473–487, 1991.

[2] S. Matsumura and K. Yamazaki, "Eurasian subarctic summer climate in response to anomalous snow cover," *Journal of Climate*, vol. 25, no. 4, pp. 1305–1317, 2012.

[3] Z. Wang and X. Zeng, "Evaluation of snow albedo in land models for weather and climate studies," *Journal of Applied Meteorology and Climatology*, vol. 49, no. 3, pp. 363–380, 2010.

[4] D. Rechid, T. J. Raddatz, and D. Jacob, "Parameterization of snow-free land surface albedo as a function of vegetation phenology based on MODIS data and applied in climate modelling," *Theoretical and Applied Climatology*, vol. 95, no. 3-4, pp. 245–255, 2009.

[5] X. Qu and A. Hall, "What controls the strength of snow-albedo feedback?" *Journal of Climate*, vol. 20, no. 15, pp. 3971–3981, 2007.

[6] X. Qu and A. Hall, "Assessing snow albedo feedback in simulated climate change," *Journal of Climate*, vol. 19, no. 11, pp. 2617–2630, 2006.

[7] F. Yang, A. Kumar, W. Wang, H.-M. H. Juang, and M. Kanamitsu, "Snow-Albedo feedback and seasonal climate variability over North America," *Journal of Climate*, vol. 14, no. 22, pp. 4245–4248, 2001.

[8] S. Matsumura and T. Sato, "Snow/ice and cloud responses to future climate change around Hokkaido," *SOLA*, vol. 7, pp. 205–208, 2011.

[9] A. Hall and X. Qu, "Using the current seasonal cycle to constrain snow albedo feedback in future climate change," *Geophysical Research Letters*, vol. 33, no. 3, Article ID L03502, 2006.

[10] J. Cohen and D. Rind, "The effect of snow cover on the climate," *Journal of Climate*, vol. 4, no. 7, pp. 689–706, 1991.

[11] T. P. Barnett, L. Dumenil, U. Schlese, E. Roeckner, and M. Latif, "The effect of Eurasian snow cover on regional and global climate variations," *Journal of the Atmospheric Sciences*, vol. 46, no. 5, pp. 661–685, 1989.

[12] S. Vavrus, "The role of terrestrial snow cover in the climate system," *Climate Dynamics*, vol. 29, no. 1, pp. 73–88, 2007.

[13] H. Douville, "Relative contribution of soil moisture and snow mass to seasonal climate predictability: a Pilot Study," *Climate Dynamics*, vol. 34, no. 6, pp. 797–818, 2010.

[14] J. W. Pomeroy, D. M. Gray, K. R. Shook et al., "An evaluation of snow accumulation and ablation processes for land surface modelling," *Hydrological Processes*, vol. 12, no. 15, pp. 2339–2367, 1998.

[15] J. P. Hardy, R. E. Davis, R. Jordan et al., "Snow ablation modeling at the stand scale in a boreal jack pine forest," *Journal of Geophysical Research D: Atmospheres*, vol. 102, no. 24, pp. 29397–29405, 1997.

[16] T. E. Link and D. Marks, "Point simulation of seasonal snow cover dynamics beneath boreal forest canopies," *Journal of Geophysical Research D: Atmospheres*, vol. 104, no. 22, pp. 27841–27857, 1999.

[17] N. R. Hedstrom and J. W. Pomeroy, "Measurements and modelling of snow interception in the boreal forest," *Hydrological Processes*, vol. 12, no. 10-11, pp. 1611–1625, 1998.

[18] V. Mahat and D. G. Tarboton, "Representation of canopy snow interception, unloading and melt in a parsimonious snowmelt model," *Hydrological Processes*, vol. 28, no. 26, pp. 6320–6336, 2013.

[19] A. Lundberg, Y. Nakai, H. Thunehed, and S. Halldin, "Snow accumulation in forests from ground and remote-sensing data," *Hydrological Processes*, vol. 18, no. 10, pp. 1941–1955, 2004.

[20] M. Stähli, T. Jonas, and D. Gustafsson, "The role of snow interception in winter-time radiation processes of a coniferous sub-alpine forest," *Hydrological Processes*, vol. 23, no. 17, pp. 2498–2512, 2009.

[21] P. Storck, D. P. Lettenmaier, and S. M. Bolton, "Measurement of snow interception and canopy effects on snow accumulation and melt in a mountainous maritime climate, Oregon, United States," *Water Resources Research*, vol. 38, no. 1, pp. 5-1–5-16, 2002.

[22] T. Yamazaki, H. Yabuki, and T. Ohata, "Hydrometeorological effects of intercepted snow in an eastern Siberian taiga forest using a land-surface model," *Hydrological Processes*, vol. 21, no. 9, pp. 1148–1156, 2007.

[23] L. C. Bowling, D. P. Lettenmaier, B. Nijssen et al., "Simulation of high-latitude hydrological processes in the Torne-Kalix basin: PILPS Phase 2(e) 1: Experiment description and summary intercomparisons," *Global and Planetary Change*, vol. 38, no. 1-2, pp. 1–30, 2003.

[24] A. Lundberg and H. Koivusalo, "Estimating winter evaporation in boreal forests with operational snow course data," *Hydrological Processes*, vol. 17, no. 8, pp. 1479–1493, 2003.

[25] J. R. Gustafson, P. D. Brooks, N. P. Molotch, and W. C. Veatch, "Estimating snow sublimation using natural chemical and isotopic tracers across a gradient of solar radiation," *Water Resources Research*, vol. 46, no. 12, Article ID W12511, 2010.

[26] O. Schulz and C. de Jong, "Snowmelt and sublimation: field experiments and modelling in the High Atlas Mountains of Morocco," *Hydrology and Earth System Sciences*, vol. 8, no. 6, pp. 1076–1089, 2004.

[27] M.-K. Woo and M. A. Giesbrecht, "Simulation of snowmelt in a subarctic spruce woodland. 1. Tree model," *Water Resources Research*, vol. 36, no. 8, pp. 2275–2285, 2000.

[28] R. Essery and P. Etchevers, "Parameter sensitivity in simulations of snowmelt," *Journal of Geophysical Research D: Atmospheres*, vol. 109, no. 20, Article ID D20111, 15 pages, 2004.

[29] L. Li and J. W. Pomeroy, "Probability of occurrence of blowing snow," *Journal of Geophysical Research D: Atmospheres*, vol. 102, no. 18, pp. 21955–21964, 1997.

[30] A. G. Price and T. Dunne, "Energy balance computations of snowmelt in a subarctic area," *Water Resources Research*, vol. 12, no. 4, pp. 686–694, 1976.

[31] J. Jin and L. Wen, "Evaluation of snowmelt simulation in the Weather Research and Forecasting model," *Journal of Geophysical Research D: Atmospheres*, vol. 117, no. 10, Article ID D10110, 2012.

[32] M. A. Giesbrecht and M.-K. Woo, "Simulation of snowmelt in a subarctic spruce woodland: 2. Open woodland model," *Water Resources Research*, vol. 36, no. 8, pp. 2287–2295, 2000.

[33] J. L. Foster, C. Sun, J. P. Walker et al., "Quantifying the uncertainty in passive microwave snow water equivalent observations," *Remote Sensing of Environment*, vol. 94, no. 2, pp. 187–203, 2005.

[34] G. E. Liston and C. A. Hiemstra, "The changing cryosphere: pan-arctic snow trends (1979–2009)," *Journal of Climate*, vol. 24, no. 21, pp. 5691–5712, 2011.

[35] M. M. Rienecker, M. J. Suarez, R. Gelaro et al., "MERRA: NASA's modern-era retrospective analysis for research and applications," *Journal of Climate*, vol. 24, no. 14, pp. 3624–3648, 2011.

[36] S. Stuefer, D. L. Kane, and G. E. Liston, "*In situ* snow water equivalent observations in the US arctic," *Hydrology Research*, vol. 44, no. 1, pp. 21–34, 2013.

[37] M. Sturm, B. Taras, G. E. Liston, C. Derksen, T. Jonas, and J. Lea, "Estimating snow water equivalent using snow depth data and climate classes," *Journal of Hydrometeorology*, vol. 11, no. 6, pp. 1380–1394, 2010.

[38] R. H. Reichle, R. D. Koster, G. J. M. de Lannoy et al., "Assessment and enhancement of MERRA land surface hydrology estimates," *Journal of Climate*, vol. 24, no. 24, pp. 6322–6338, 2011.

[39] B. J. Peterson, R. M. Holmes, J. W. McClelland et al., "Increasing river discharge to the Arctic Ocean," *Science*, vol. 298, no. 5601, pp. 2171–2173, 2002.

[40] M. A. Rawlins, H. Ye, D. Yang, A. Shiklomanov, and K. C. McDonald, "Divergence in seasonal hydrology across Northern Eurasia: emerging trends and water cycle linkages," *Journal of Geophysical Research*, vol. 114, no. D18, 2009.

[41] L. Kitaev, A. Kislov, A. Krenke, V. Razuvaev, R. Martuganov, and I. Konstantinov, "The snow cover characteristics of northern Eurasia and their relationship to climatic parameters," *Boreal Environment Research*, vol. 7, no. 4, pp. 437–445, 2002.

[42] Y. Iijima, A. N. Fedorov, H. Park et al., "Abrupt increases in soil temperatures following increased precipitation in a permafrost region, central Lena River basin, Russia," *Permafrost and Periglacial Processes*, vol. 21, no. 1, pp. 30–41, 2010.

[43] K. Suzuki, J. Kubota, T. Ohata, and V. Vuglinsky, "Influence of snow ablation and frozen ground on spring runoff generation in the Mogot Experimental Watershed, southern mountainous taiga of eastern Siberia," *Nordic Hydrology*, vol. 37, no. 1, pp. 21–29, 2006.

[44] K. Suzuki, E. Konohira, Y. Yamazaki, J. Kubota, T. Ohata, and V. Vuglinsky, "Transport of organic carbon from the Mogot Experimental Watershed in the southern mountainous taiga of eastern Siberia," *Nordic Hydrology*, vol. 37, no. 3, pp. 303–312, 2006.

[45] Y. Zhang, K. Suzuki, T. Kadota, and T. Ohata, "Sublimation from snow surface in southern mountain taiga of eastern Siberia," *Journal of Geophysical Research D: Atmospheres*, vol. 109, no. 21, 2004.

[46] K. Suzuki, J. Kubota, Y. Zhang, T. Kadota, T. Ohata, and V. Vuglinsky, "Snow ablation in an open field and larch forest of the southern mountainous region of eastern Siberia," *Hydrological Sciences Journal*, vol. 51, no. 3, pp. 465–480, 2006.

[47] D. B. Gesch, K. L. Verdin, and S. K. Greenlee, "New land surface digital elevation model covers the earth," *Eos*, vol. 80, no. 6, pp. 69–70, 1999.

[48] E. Bartholomé and A. S. Belward, "GLC2000: a new approach to global land cover mapping from earth observation data," *International Journal of Remote Sensing*, vol. 26, no. 9, pp. 1959–1977, 2005.

[49] R. Suzuki, V. Razuvaev, O. N. Bulygina, and T. Ohata, *Baseline Meteorological Data in Siberia (BMDS) Version 4.1*, Institute of Observational Research for Global Change, Japan Agency for Marine-Earth Science and Technology, Yokosuka, Japan, 2007.

[50] D. Yang and T. Ohata, "A bias-corrected Siberian regional precipitation climatology," *Journal of Hydrometeorology*, vol. 2, no. 2, pp. 122–139, 2001.

[51] G. E. Liston and K. Elder, "A meteorological distribution system for high-resolution terrestrial modeling (MicroMet)," *Journal of Hydrometeorology*, vol. 7, no. 2, pp. 217–234, 2006.

[52] G. E. Liston and K. Elder, "A distributed snow-evolution modeling system (snowmodel)," *Journal of Hydrometeorology*, vol. 7, no. 6, pp. 1259–1276, 2006.

[53] G. E. Liston and C. A. Hiemstra, "A simple data assimilation system for complex snow distributions (SnowAssim)," *Journal of Hydrometeorology*, vol. 9, no. 5, pp. 989–1004, 2008.

[54] M. Sturm, J. Holmgren, and G. E. Liston, "A seasonal snow cover classification system for local to global applications," *Journal of Climate*, vol. 8, no. 5, pp. 1261–1283, 1995.

[55] G. E. Liston and D. K. Hall, "An energy-balance model of lake-ice evolution," *Journal of Glaciology*, vol. 41, no. 138, pp. 373–382, 1995.

[56] G. E. Liston, R. B. Haehnel, M. Sturm, C. A. Hiemstra, S. Berezovskaya, and R. D. Tabler, "Simulating complex snow distributions in windy environments using SnowTran-3D," *Journal of Glaciology*, vol. 53, no. 181, pp. 241–256, 2007.

[57] K. Suzuki, Y. Kodama, T. Nakai et al., "Impact of land-use changes on snow in a forested region with heavy snowfall in Hokkaido, Japan," *Hydrological Sciences Journal*, vol. 56, no. 3, pp. 443–467, 2011.

[58] K. Suzuki, Y. Kodama, Y. Takeshi, K. Kosugi, and Y. Nakai, "Snow accumulation on evergreen needle-leaved and deciduous broad-leaved trees," *Boreal Environment Research*, vol. 13, no. 5, pp. 403–416, 2008.

[59] D. K. Hall, G. A. Riggs, V. V. Salomonson, N. E. DiGirolamo, and K. J. Bayr, "MODIS snow-cover products," *Remote Sensing of Environment*, vol. 83, no. 1-2, pp. 181–194, 2002.

[60] S. L. Barnes, "A technique for maximizing details in numerical weather map analysis," *Journal of Applied Meteorology*, vol. 3, no. 4, pp. 396–409, 1964.

[61] X. Ma, Y. Fukushima, T. Hiyama, T. Hashimoto, and T. Ohata, "A macro-scale hydrological analysis of the Lena River basin," *Hydrological Processes*, vol. 14, no. 3, pp. 639–651, 2000.

[62] A. G. Klein and A. C. Barnett, "Validation of daily MODIS snow cover maps of the Upper Rio Grande River Basin for the 2000-2001 snow year," *Remote Sensing of Environment*, vol. 86, no. 2, pp. 162–176, 2003.

[63] J. W. Pomeroy and R. L. H. Essery, "Turbulent fluxes during blowing snow: field tests of model sublimation predictions," *Hydrological Processes*, vol. 13, no. 18, pp. 2963–2975, 1999.